Neurotherapeutics (2021) 18:326–339
https://doi.org/10.1007/s13311-020-00943-1

ORIGINAL ARTICLE

Levistolide A Attenuates Alzheimer's Pathology Through Activation of the PPARγ Pathway

Xiaodan Qu[1] · Peipei Guan[1] · Li Han[1] · Zhanyou Wang[2] · Xueshi Huang[1]

Accepted: 1 October 2020 / Published online: 9 October 2020

Abstract

Alzheimer's disease (AD) is a neurodegenerative disease characterized by β-amyloid (Aβ) protein deposition, neurofibrillary tangle (NFT) formation, and neuronal loss in the brain. The current study was designed to investigate the potential mechanisms by which levistolide A affects the pathogenesis of AD in an amyloid precursor protein/presenilin 1 (APP/PS1) transgenic (Tg) mouse model of AD and N2a/APP695swe cells. Specifically, behavioral changes in levistolide A–treated APP/PS1 Tg mice were assessed by the nest-building and Morris water maze (MWM) tests. Levistolide A treatment clearly ameliorated memory deficits and cognitive decline in APP/PS1 Tg mice. Aβ generation and the inflammatory response in APP/PS1 Tg mouse brains were clearly reduced after long-term levistolide A application. Mechanistically, levistolide A concurrently stimulated the expression of α-secretase and decreased the generation of β- and γ-secretases. In addition, levistolide A inhibited the phosphorylation of tau in the brains of the Tg mice. Furthermore, *in vitro* and *in vivo* experiments suggested that peroxisome proliferator–activated receptor γ (PPARγ) is the key transcription factor that mediates the regulatory effects of levistolide A on the expression of α-, β-, and γ-secretases and phosphorylation of tau. Collectively, these findings show that levistolide A may be a candidate for the treatment of AD.

Key Words Alzheimer's disease · levistolide A · β-amyloid protein · tau phosphorylation · PPARγ · GSK-3β

Introduction

Alzheimer's disease (AD) is becoming a severe financial, social, and healthcare burden throughout the world. A progressive neurodegenerative disease, AD is characterized by the abnormal production and deposition of the peptide β-amyloid (Aβ) and the hyperphosphorylation of tau [1–3]. Consequent Aβ accumulation can cause multiple types of neuronal injury by initiating oxidative stress and inflammation, resulting in the cognitive decline observed in AD [4, 5]. Similarly, the tau protein is another key regulator of AD whose phosphorylation and proteolysis are closely associated with the disease [6]. In addition, hyperphosphorylated tau can assemble to form paired helical filaments, which are deposited in the form of neurofibrillary tangles (NFTs). The formation of NFTs can induce neuronal apoptosis or death. Therefore, reducing the formation and aggregation of Aβ and phosphorylated tau may be beneficial for improving the symptoms of AD.

Peroxisome proliferator–activated receptor γ (PPARγ) plays a protective role in the central nervous system (CNS) [7]. For example, PPARγ agonists have been observed to reduce the level of Aβ, by either reducing the production of Aβ or enhancing Aβ clearance [8]. Aβ is derived from the amyloidogenic pathway by the sequential cleavage of amyloid precursor protein (APP) with β-secretase (BACE-1) and γ-secretase [9–11]. In contrast, in the nonamyloidogenic pathway, the production of Aβ is inhibited due to the cleavage of APP with α-secretase, producing soluble amyloid precursor protein α (sAPPα) [12]. Regarding the regulation of these pathways, evidence shows that PPARγ can suppress the expression of β-site APP cleaving enzyme 1 (BACE1), resulting in the production of Aβ [13]. In addition, thiazolidinedione, a PPARγ agonist, has been shown to inhibit the production of Aβ by reducing the release of γ-secretase [14], although the

✉ Li Han
hanli@mail.neu.edu.cn

✉ Zhanyou Wang
wangzy@cmu.edu.cn

[1] Institute of Microbial Pharmaceuticals, College of Life and Health Sciences, Northeastern University, Shenyang 110819, People's Republic of China

[2] Institute of Health Sciences, China Medical University, Shenyang 110122, People's Republic of China

mechanism by which PPARγ downregulates the expression of γ-secretase has not been clearly revealed.

Involved in the phosphorylation of tau, glycogen synthase kinase-3β (GSK-3β) is one of the main tau kinases during the course of AD development and progression [12]. GSK-3β can phosphorylate tau at the sites Thr181 and Ser396 [15, 16]. Moreover, PPARγ has been proven to mitigate the activity of GSK-3β in stimulating the hyperphosphorylation of tau, consequently improving the progression of AD [17–19].

In addition to Aβ and tau, neuroinflammation plays a significant role in the pathogenesis of dementia [20]. By activating astrocytes and microglia, aggregated forms of Aβ and tau can increase the expression of inflammatory cytokines, such as interleukin-6 (IL-6), interleukin-1β (IL-1β), and tumor necrosis factor alpha (TNF-α) [21–24], which slows the progression of AD. During the course of this process, PPARγ downregulates the synthesis of cyclooxygenase-2 (COX-2), inducible nitric oxide synthase (iNOS), and proinflammatory cytokines through nuclear factor (NF)-κB. Treatment with PPARγ agonists has been proven to deactivate glial cells by decreasing the production of inflammatory cytokines [25].

Levistolide A is a characteristic phthalide constituent of the Umbelliferae family of medicinal plants, including *Angelicae sinensis* and *Ligusticum chuanxiong* [26, 27]. Previous studies have shown that levistolide A has multiple biological activities, such as its induction of olfactory neuron regeneration and anti-inflammatory effects [28–31]. When screening bioactive compounds from a traditional Chinese medicine for the treatment of AD, we found that levistolide A improved the learning ability of APP/PS1 transgenic (Tg) mice. Based on these observations, the effect of levistolide A on the production and deposition of Aβ and the hyperphosphorylation of tau and the underlying mechanisms of levistolide A were investigated *in vitro* and *in vivo*.

Materials and Methods

Animals and Treatments

APP/PS1 Tg mice were obtained from the Jackson Laboratory (Bar Harbor, ME, USA). Twelve 6-month-old female mice were randomly divided into two groups (6 in the vehicle-treated group, and 6 in the levistolide A-treated group). The levistolide A used in this study was isolated from *Ligusticum chuanxiong* in our laboratory. The purity of the isolated levistolide A was greater than 98.0%, as determined by high-pressure liquid chromatography (HPLC). Mice from the levistolide A–treated group received an intraperitoneal injection of levistolide A (2 mg kg^{-1}) every other day, and those from the control group were treated with vehicle (sterile water with 60% v/v 1,2-propanediol). After 4 months, the mice were subjected to behavioral experiments. Then, the brains of the mice in different groups were collected after anesthetization and perfusion. Just before sacrifice, sera were collected from the retrobulbar venous plexus for subsequent assessment.

Morris Water Maze Test

The effect of levistolide A on the spatial learning and memory abilities of the mice was assessed using the Morris water maze (MWM) test. First, the mice underwent visible platform training for 2 consecutive days (four trials per day). Then, the platform was submerged 1 cm below the surface of the water, and milk was added to the water to hide the platform. The mice were permitted a maximum time of 60 s to find and 15 s to stay on the hidden platform, starting from their release in a randomly chosen quadrant. If the mouse failed to locate the platform within 60 s, it was guided to the platform and allowed to stay on the platform for 15 s. This navigation test was carried out over 5 days. On each testing day, the animals performed 4 trials separated by 30-min intervals. The latency time and path length to find the hidden platform were recorded to calculate their spatial learning scores. After the navigation test, the platform was removed, and a probe trial was performed to assess the memory abilities of the mice. The mice were permitted to swim freely for 60 s, and the number of times that the mice crossed the location of the platform was recorded. All of the data were analyzed with a computer program (SMART 3.0, Panlab, Barcelona, Spain).

Nest-Building Test

To assess the social behavior of the animals, the nest-building test was carried out. Briefly, the mice were individually fed in each cage. Eight square pieces of A4 paper (5 × 5 cm^2) were placed in each cage. Changes in the pieces of paper were simultaneously observed for 6 days through photographic recording. Nest-building ability was assessed based on the following 4-point system: (1) no biting/tearing of the paper with random dispersion of the paper; (2) no biting/tearing of the paper with gathering of the paper in a corner/side of the cage; (3) moderate biting/tearing of the paper with gathering of the paper in a corner/side of the cage; and (4) extensive biting/tearing of the paper with gathering of the paper in a corner/side of the cage.

Immunofluorescence Staining

Double immunofluorescence staining was carried out to observe the colocalization of Aβ, glial fibrillary acidic protein (GFAP), and ionized calcium-binding adaptor molecule 1 (Iba-1) in brain tissue. Frozen brain sections (10 μm) were incubated with mouse anti-Aβ (1:200, Santa Cruz Biotechnology, sc-28365) and rabbit anti-GFAP (1:100, Abcam, ab7260) primary antibodies or mouse anti-Aβ (1:

200, Santa Cruz Biotechnology, sc-28365) and rabbit anti-Iba-1 (1:100, Abcam, 153696) primary antibodies overnight at 4 °C. Fluorescein isothiocyanate-conjugated goat anti-mouse IgG (1:200, Thermo Fisher Scientific, A32723) and goat anti-rabbit IgG (1:200, Thermo Fisher Scientific, A32732) secondary antibodies were used to incubate the sections for 2 h at room temperature. The nuclei were counterstained by incubation in 1 μg/mL 4′,6-diamidino-2-phenylindole (DAPI) for 5 min, followed by extensive washing in distilled water. Images were acquired using a confocal laser scanning microscope (SP8, Leica).

Immunofluorescence staining was used to analyze the nuclear translocation of PPARγ in cells. N2a/APP695swe cells were plated on a coverslip at a density of 1×10^6 cells/mL. After the indicated treatment, the cells were washed with phosphate-buffered saline (PBS, 0.01 M, pH = 7.2–7.4), fixed with 4% paraformaldehyde at 37 °C for 15 min and then preincubated with 5% BSA in PBS with 0.3% v/v Tween-20 (PBST) at 37 °C for 60 min. After preincubation, the cells were incubated with anti-PPARγ antibody (1:200 in Tris-buffered saline (TBS, 1 ×, pH = 7.6)) at 4 °C overnight. They were then further incubated with an Alexa Fluor 488–conjugated goat anti-rabbit antibody (1:500, Beyotime Biotechnology, Shanghai, China) for 1 h. The cell nuclei were counterstained with Hoechst 33342 (Beyotime Biotechnology, Shanghai, China) for 3 min in the dark. Images were captured using a confocal laser scanning microscope (SP8, Leica); green fluorescence indicates PPARγ, and blue fluorescence indicates nuclei. The fluorescence intensities were analyzed by using ImageJ software.

Immunohistochemical Staining

Standard avidin-biotinylated complex immunohistochemical (IHC) staining was performed to analyze the distribution of Aβ plaques in the brains of APP/PS1 Tg mice. Briefly, paraffin-embedded brain tissue samples were sectioned into 5-μm-thick slices that were then successively dewaxed, rehydrated, and stained as previously described [32]. Mouse anti-Aβ primary antibody (1:500; Sigma) and biotinylated goat anti-mouse IgG (1:200) were used for staining. Quantitative analysis of Aβ plaques was performed by using Image-Pro Plus 6.0 software. The numbers and areas of Aβ-positive plaques in the cortex and hippocampus were analyzed.

N2a/APP695swe Cell Culture and Treatment

N2a/APP695swe cells stably expressing the Swedish mutant human APP695 gene were provided as a gift from the laboratory of Prof. Hua-Xi Xu (Xiamen University). Cells were cultured in high-glucose Dulbecco's modified Eagle's medium (DMEM, Gibco, Carlsbad, CA, USA) supplemented with 10% (v/v) fetal bovine serum (FBS, Gibco), 1% (v/v) glutamine (Biological Industries), 1% (v/v) penicillin-streptomycin (Biological Industries), and 2 mg/mL (m/v) G418 (Sigma, St. Louis, MO, USA) at 37 °C under an atmosphere of 5% CO_2. To assess cell viability during prolonged incubation with levistolide A, the 3-(4,5-dimethylthiazol-2-yl)-2,5-diphenyltetrazolium bromide (MTT) assay was performed. Cells were treated with serial dilutions of levistolide A ranging in concentration from 0 to 10 μg/mL for 24 h prior to lysis with ice-cold radioimmunoprecipitation assay (RIPA) buffer (Beyotime Biotechnology, Shanghai, China) containing a protease inhibitor cocktail (Promega Corporation, Madison, Wisconsin, USA) and phosphatase inhibitor cocktail (CWBIO, Beijing, China). In addition, the cells were exposed to GW9662 (2-chloro-5-nitro-N-phenylbenzamide, 30 μM, GW, MedChem Express, Princeton, New Jersey, USA) for 1 h prior to levistolide A treatment (0–10 μg/mL) for 24 h to determine whether the PPARγ pathway is involved in the effects of levistolide A on AD.

Sandwich Enzyme-Linked Immunosorbent Assay

To detect $A\beta_{1-40}$ and $A\beta_{1-42}$, homogenates of cerebral cortex tissues and the sera of APP/PS1 Tg mice were prepared, and the supernatants of N2a/APP695swe cells and lysed N2a/APP695swe cells were collected. The samples were diluted with dilution buffer at the appropriate ratio, immediately added to 96-well plates, and analyzed using enzyme-linked immunosorbent assay (ELISA) kits (MSKBIO, China; $A\beta_{1-40}$, kt99164; $A\beta_{1-42}$, cx20056) according to the manufacturer's instructions. The absorbance at a wavelength of 450 nm was recorded using a microplate reader.

Western Blot Analysis

Western blot analysis was used to evaluate protein expression in protein extracts from the mouse brains and cultured cells. The cerebral cortical tissues of the mice were immersed in ice-cold RIPA lysis buffer containing protease and phosphatase inhibitor cocktail. After homogenization by sonication, the mixtures were centrifuged at 13000 rpm for 30 min at 4 °C, and the supernatants were collected. Cells were washed twice with ice-cold PBS and then lysed in 80 μL of RIPA buffer containing protease and phosphatase inhibitors. Cells were homogenized in RIPA buffer at 4 °C before centrifugation at 13000 rpm for 30 min to collect the supernatants. The supernatants were used for western blotting. Equal amounts of protein were loaded in each well for sodium dodecyl sulfate-polyacrylamide gel electrophoresis (SDS-PAGE), and the separated proteins were then blotted onto polyvinylidene fluoride (PVDF) membranes (Millipore, Temecula, CA, USA). After blocking with 2.5% nonfat milk in TBS (1 ×) with 0.1% v/v Tween-20 (TBST) buffer for 30 min at room temperature, each membrane was probed overnight at 4 °C with

the following specific primary antibodies: mouse anti-Aβ (1:1000, Santa Cruz Biotechnology, sc-28365), rabbit anti-A disintegrin and metalloproteinase 10 (ADAM10, 1:1000, CST, 14194), rabbit anti-TNF-α-converting enzyme (TACE orADAM17, 1:1000, Abcam, ab2051), rabbit anti-BACE1 (1:1000, Abcam, ab183612), rabbit anti-Presenilin 1 (PS1, 1:1000, CST, 5643), rabbit anti-Presenilin 2 (PS2, 1:1000, CST, 9979), rabbit anti- Nicastrin (NCT, 1:1000, CST, 5665), mouse anti-sAPPα (1:1000, Immuno-Biological Laboratories (IBL), 11088), mouse anti-soluble amyloid precursor β (sAPPβ, 1:1000, IBL, 10321), mouse anti-tau (1:2000, CST, 4019), rabbit anti-phospho-tau (Thr181) (1:2000, CST, 12885), rabbit anti-phospho-tau (Ser416) (1:2000, CST, 15013), mouse anti-phospho-tau (Ser396) (1:1000, CST, 9632), rabbit anti-phospho-GSK 3α/β (Ser21/Ser9) (1:2000, CST, 9327), rabbit anti-GSK3α/β (1:2000, CST, 5676), rabbit anti-GFAP (1:1000, CST, 80788), rabbit anti-Iba1 (1:1000, CST, 17198), rabbit anti-IL-1β (1:1000, Santa Cruz, sc-7884), rabbit anti-IL-6 (1:1000, CST, 12153), mouse anti-TNF-α (1:1000, Santa Cruz, sc-52,746), rabbit anti-postsynaptic density proteins 95 (PSD95, 1:1000, CST, 3409), mouse anti-synaptophysin (SYP, 1:1000, Santa Cruz, sc-365488), rabbit anti-PPARγ (1:2000, CST, 2443), rabbit anti-GAPDH (1:3000, CST, 5174), and rabbit anti-β-actin (1:3000, CST, 4970). The membranes were then incubated with horseradish peroxidase–conjugated secondary antibody (1:10000 in TBST) for 1 h at room temperature. Visualization of the immunoreactive bands was performed using a Bio-Rad system with enhanced chemiluminescence (ECL), and grayscale analysis was performed using ImageJ software. The intensity of each protein band was normalized to that of the corresponding band for β-actin or GAPDH, and the relative value was then normalized to that of the vehicle group.

Statistical Analyses

All values are presented as the mean ± standard deviation (S.D.). One-way analysis of variance (ANOVA) or Student's *t* test was used to evaluate differences among more than three groups or differences between two groups, respectively. All data were analyzed using GraphPad Prism software, and differences were assumed to be highly statistically significant at $p < 0.01$ and statistically significant at $p < 0.05$.

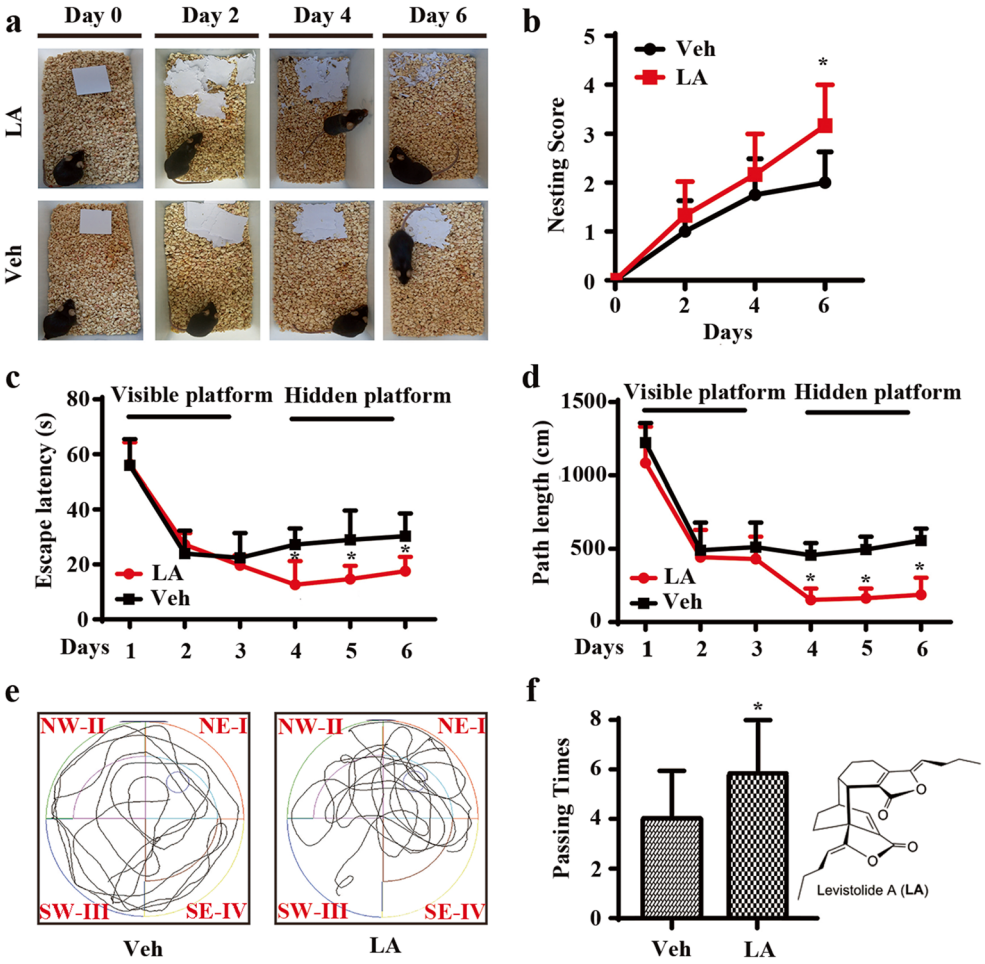

Fig. 1 Levistolide A treatment rescued the memory deficits and cognitive disorders in APP/PS1 Tg mice. (a) Results of the nest-building test in the APP/PS1 Tg mice. (b) Statistical analysis of nest score for each group of mice. (c) Escape latency in the visible platform and hidden platform test. (d) Path length in the visible platform and hidden platform test. (e) Representative escape routes on the last day of the hidden platform test are shown. (f) Number of times crossing the center region without the platform in 1 min. Data represent the mean ± SD ($n > 3$), $^*p < 0.05$ compared with the vehicle-treated APP/PS1 Tg mice

Results

Levistolide A Treatment Rescued Memory Deficits and Cognitive Disorders in APP/PS1 Tg Mice

APP/PS1 Tg mice are widely used in AD-related studies, including pharmacodynamic evaluations and evaluations of underlying mechanisms. To investigate the effects of levistolide A on AD, we first determined its effects on the learning ability of APP/PS1 Tg mice with the nest-building and MWM tests. The results of the nest-building test demonstrated that the nesting scores of the levistolide A–treated mice were significantly higher than those of the vehicle-treated controls (Fig. 1a, b), suggesting the ability of levistolide A to rescue the impairment of social behavior in APP/PS1 Tg mice. To further validate the above observation, the MWM test was carried out to determine the learning ability of APP/PS1 Tg mice. The results demonstrated significant difference in learning ability between the levistolide A– and vehicle-treated mice over the first 2 days of training tests. In contrast, levistolide A clearly shortened the time taken and distance traveled for the mice to find the hidden platform in subsequent experiments (Fig. 1c, d). In the spatial probe trial, the time taken to cross the original platform was clearly elevated in the levistolide A–treated group compared to that of the control group (Fig. 1e, f). Based on these observations, the spatial learning and memory

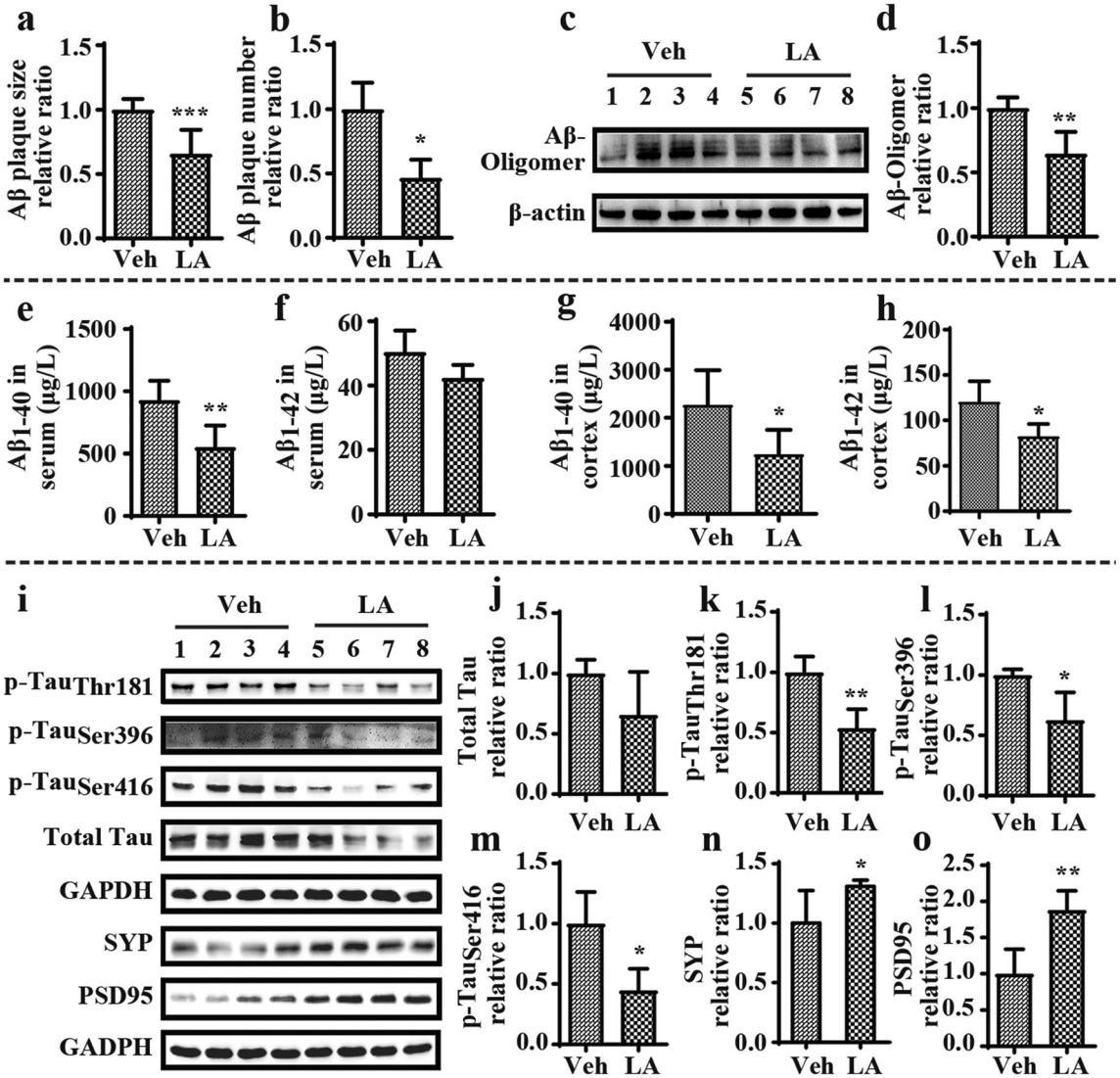

Fig. 2 Levistolide A decreased the Aβ generation and deposition and reduced the expression of phosphorylation of tau protein and loss of synapses in APP/PS1 Tg mice. (a, b) Quantitative analysis of Aβ immunohistochemistry staining in the brains of APP/PS1 Tg mice. (c, d) Expression levels of Aβ oligomer protein in the cortex tissue of APP/PS1 Tg mice. β-actin was used as internal control. (e, f) Expression levels of $A\beta_{1–40}$ and $A\beta_{1–42}$ in the serum of APP/PS1 Tg mice. (g, h) Expression levels of $A\beta_{1–40}$ and $A\beta_{1–42}$ in the cortex tissue of APP/PS1 Tg mice. (i) Western blots showing the protein levels, including total tau, p-tau (Thr181, Ser396, Ser416), SYP, and PSD95. GAPDH was used as internal control. (j–o) Quantitative analysis of the results shown in **i**. Data represent the mean ± SD ($n > 3$), $^{*}p < 0.05$, $^{**}p < 0.01$, compared with the vehicle-treated APP/PS1 Tg mice

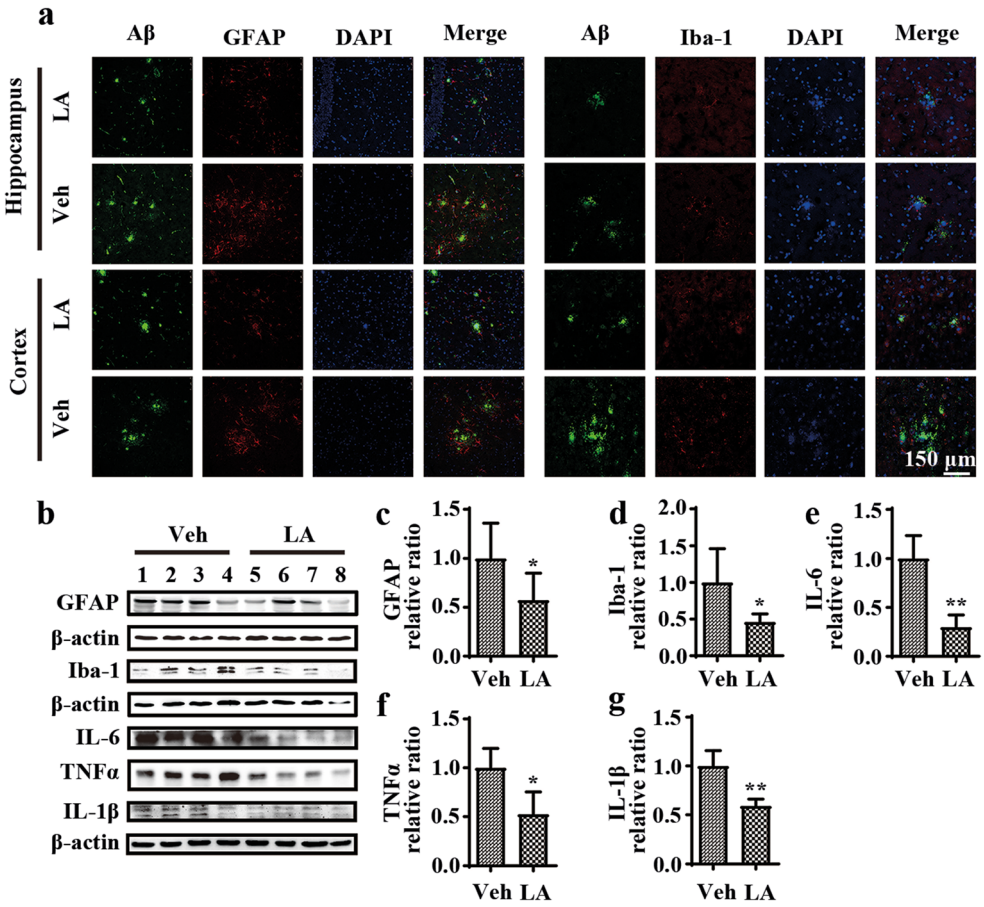

Fig. 3 Levistolide A mitigated activation of Aβ-accompanied glial cells in APP/PS1 Tg mice. (a) Double immunofluorescence staining analyzed the distribution and expression of Aβ with GFAP and Iba-1 in cortex and hippocampus of APP/PS1 Tg mice brains. (b) Western blot detection of GFAP, Iba-1, IL-6, IL-1β, and TNF-α in the cortex of APP/PS1 Tg mice. β-actin was used as internal control. (c–g) Quantitative analysis of the immunoreactivities to the antibodies presented in the previous panel. Data represent the mean ± SD ($n > 3$), *$p < 0.05$, **$p < 0.01$, compared with the vehicle-treated APP/PS1 Tg mice

abilities of the mice were improved by treatment with levistolide A.

Levistolide A Treatment Decreased the Aggregation of Aβ in APP/PS1 Tg Mice

In view of the essential roles of Aβ in AD, IHC staining was carried out to reveal the effect of levistolide A on the generation and aggregation of Aβ in the brains of APP/PS1 Tg mice. The results showed that the numbers of immunoreactive amyloid plaques (APs) in the hippocampus and cerebral cortices of levistolide A–treated mice were significantly decreased compared to those of vehicle-treated mice (Fig. 2a, b). The effect of levistolide A on Aβ production and the levels of Aβ oligomers were simultaneously assessed using ELISA and western blotting, respectively. The results showed that the level of Aβ oligomers was dramatically reduced in levistolide A–treated mice compared to vehicle-treated mice (Fig. 2c, d). Similarly, levistolide A treatment dramatically reduced the production of soluble $Aβ_{1–40}$ and $Aβ_{1–42}$ in the sera and cortical tissues of APP/PS1 Tg mice (Fig. 2e–h). Taken together, our results revealed that levistolide A efficiently suppressed the production and aggregation of Aβ in APP/PS1 Tg mice.

Levistolide A Reduced the Phosphorylation of Tau and the Loss of Synapses in APP/PS1 Tg Mice

As the predominant pathological characteristics of AD, the hyperphosphorylation and aggregation of tau were next assessed in the current study. By western blot analysis, we determined that levistolide A treatment decreased the level of tau phosphorylated at Ser396, Ser416, and Thr181 and even the total tau protein level in the cerebral cortices of APP/PS1 Tg mice (Fig. 2i–m). As levistolide A can attenuate the production of Aβ and phosphorylated tau, we then

Fig. 4 Levistolide A treatment accelerated the nonamyloidogenic APP ▶ pathway in APP/PS1 Tg mice and in N2a/APP695swe cells. (a) Western blots showing the protein levels associated with APP metabolism, including sAPPα, ADAM10, TACE, sAPPβ, BACE1, PS1, PS2, and NCT. β-actin and GAPDH were used as internal control. (b–i) Quantitative analysis of the results shown in (a). (j) Cell viability was measured by MTT assay and expressed relative to the vehicle. (k, l) Expression levels of $Aβ_{1–40}$ and $Aβ_{1–42}$ in the supernatant and lysis of N2a/APP695swe cells. (m) Western blots showing the protein levels associated with APP metabolism, including Aβ oligomer, sAPPα, ADAM10, TACE, sAPPβ, BACE1, PS1, PS2, and NCT. β-actin and GAPDH were used as internal control. (n–v) Quantitative analysis of the results shown in (m). Data represent the mean ± SD ($n > 3$), *, #$p < 0.05$, **, ##$p < 0.01$, ***, ###$p < 0.001$, compared with the vehicle

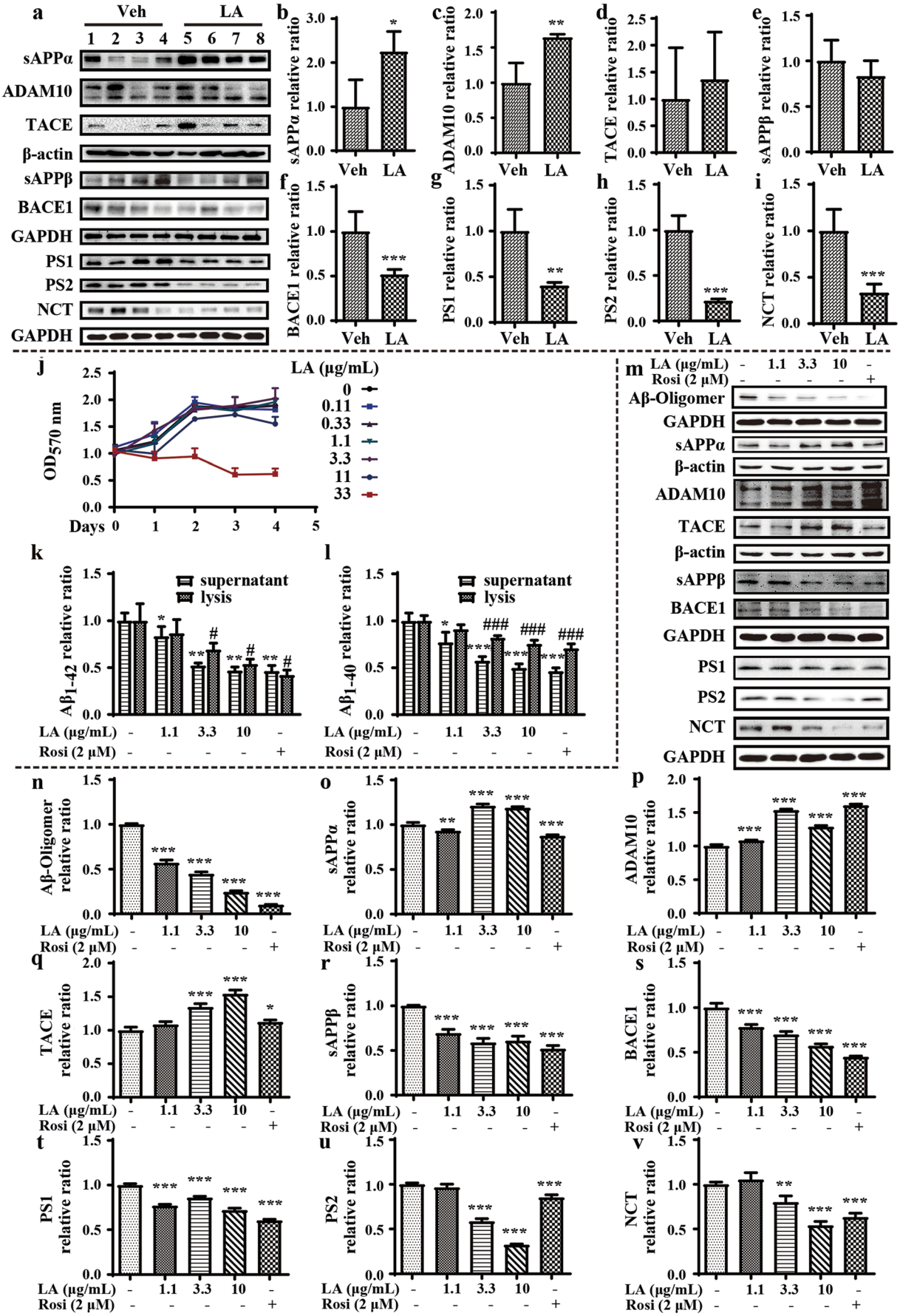
a
Veh
LA
1 2 3 4 5 6 7 8
sAPPα
ADAM10
TACE
β-actin
sAPPβ
BACE1
GAPDH
PS1
PS2
NCT
GAPDH
b sAPPα relative ratio
c ADAM10 relative ratio
d TACE relative ratio
e sAPPβ relative ratio
f BACE1 relative ratio
g PS1 relative ratio
h PS2 relative ratio
i NCT relative ratio
Veh LA
j
OD570 nm
Days
LA (μg/mL)
0
0.11
0.33
1.1
3.3
11
33
k
l
supernatant
lysis
Aβ1-42 relative ratio
Aβ1-40 relative ratio
LA (μg/mL) - 1.1 3.3 10 -
Rosi (2 μM) - - - - +
m
LA (μg/mL) - 1.1 3.3 10 -
Rosi (2 μM) - - - - +
Aβ-Oligomer
GAPDH
sAPPα
β-actin
ADAM10
TACE
β-actin
sAPPβ
BACE1
GAPDH
PS1
PS2
NCT
GAPDH
n Aβ-Oligomer relative ratio
o sAPPα relative ratio
p ADAM10 relative ratio
q TACE relative ratio
r sAPPβ relative ratio
s BACE1 relative ratio
t PS1 relative ratio
u PS2 relative ratio
v NCT relative ratio

measured its effects on the functions of synapses. By western blot analysis, we found that the levels of SYP and PSD95, characteristic proteins on the membranes of synapses, were increased in the cerebral cortices of APP/PS1 Tg mice by treatment with levistolide A (Fig. 2i, n, o). These results demonstrated that levistolide A could prevent the loss of SYP and PSD95 in the brains of APP/PS1 Tg mice.

Levistolide A Mitigated the Stimulatory Effects of Aβ on Glial Cells in APP/PS1 Tg Mice

Given the critical roles of neuroinflammation in AD [33, 34], immunofluorescence staining experiments were carried out to evaluate the effect of levistolide A on the activities of microglia and astrocytes. The results showed that positive staining for GFAP and Iba-1 was clearly attenuated in levistolide A–treated mice, especially positive staining for GFAP and Iba-1 associated with APs (Fig. 3a). Additionally, the protein levels of GFAP and Iba-1 were further verified by western blot analysis (Fig. 3b–d). As expected, the levels of GFAP and Iba-1 were decreased in levistolide A–treated mice compared to control mice. Furthermore, as activated glial cells can accelerate the process of neuroinflammation by releasing proinflammatory cytokines and other toxic mediators, we carried out experiments to analyze the production of the proinflammatory cytokines TNF-α, IL-1β, and IL-6. As shown in Fig. 3b and e–g, treatment with levistolide A attenuated the protein expression of TNF-α, IL-6, and IL-1β in APP/PS1 Tg mice. These observations revealed that levistolide A effectively attenuated the inflammatory response by suppressing the activities of microglial cells and astrocytes in APP/PS1 Tg mice.

Levistolide A Accelerated the Nonamyloidogenic Metabolism of APP *In Vitro* and *In Vivo*

To determine how levistolide A suppresses the production of Aβ, we next determined the expression of secretases. Levistolide A significantly increased the expression of ADAM10 (Fig. 4a, c), which resulted in the elevated production of sAPPα (Fig. 4a, b). In contrast, the expression level of BACE1 was noticeably decreased in levistolide A–treated APP/PS1 Tg mice compared to control mice (Fig. 4a, f), but the production of sAPPβ was not significantly affected (Fig. 4a, e). Notably, the average production of sAPPβ was attenuated by treatment with levistolide A in APP/PS1 Tg mice (Fig. 4a, e). In addition, the expression of PS1, PS2, and NCT was downregulated by levistolide A, which suggests that levistolide A can suppress the production of Aβ (Fig. 4a, g–i). To validate the above observations, similar experiments were performed in N2a/APP695swe cells. First, the toxicity of levistolide A was measured by MTT assay, the results of which demonstrated that levistolide A did not induce obvious toxicity to neuronal cells when its concentration was lower than 11 μg/mL, whereas 33 μg/mL levistolide A was extremely highly toxic to the neurons (Fig. 4j). On the basis of this observation, we treated N2a/APP695swe cells with 0–10 μg/mL levistolide A for 24 h. The results demonstrated that levistolide A treatment clearly decreased the production of $A\beta_{1-40}$ and $A\beta_{1-42}$, which is similar to the effects of rosiglitazone (Rosi, Sigma-Aldrich, St. Louis, Missouri, USA), a PPARγ agonist (Fig. 4k, l). Similar to these *in vivo* results, results obtained *in vitro* also demonstrated that levistolide A suppressed the production and aggregation of Aβ by concurrently activating α-secretases, including ADAM10 and TACE as well as decreasing the activity of β-secretase, BACE1, and γ-secretases, such as PS1, PS2, and NCT (Fig. 4m, n, p, q, s, v). These actions of levistolide A resulted in the elevated production of sAPPα and reduced the cleavage product sAPPβ in N2a/APP695swe cells (Fig. 4m, o, r).

Fig. 5 The effects of levistolide A on reducing Tau phosphorylation via GSK signaling pathway. (a, b) Expression levels of GSK-3α/β and p-GSK-3α/β protein in the cortex tissue of APP/PS1 Tg mice. GAPDH was used as internal control. Data represent the mean ± SD ($n > 3$), $^{*}p < 0.05$, $^{**}p < 0.01$, $^{***}p < 0.001$, compared with the vehicle-treated APP/PS1 Tg mice. (c, d) Western blots showing the protein levels of GSK-3α/β and p-GSK-3α/β protein in the N2a/APP695swe cells. (e) Western blots showing the protein levels including total-Tau, p-Tau (Thr181, Ser396, Ser416). GAPDH was used as internal control. (f–i). Quantitative analysis of the results shown in (e). Data represent the mean ± SD ($n > 3$), $^{*}p < 0.05$, $^{**}p < 0.01$, $^{***}p < 0.001$, compared with the vehicle

The Inhibitory Effects of Levistolide A on the Phosphorylation of Tau Occur via a GSK-Dependent Mechanism

In light of the critical roles of GSK-3α/β in the phosphorylation of tau [35, 36], we investigated its effects on levistolide A–mediated tau phosphorylation. The phosphorylation of GSK-3α/β, an inactive form of the enzyme, was dramatically elevated in the levistolide A–treated group compared to the vehicle-treated group (Fig. 5a, b). To confirm this *in vivo* observation, the effect of levistolide A on the phosphorylation of GSK-3α/β was investigated in N2a/APP695swe cells. As expected, the results revealed that the degree of GSK-3α/β phosphorylation in N2a/APP695swe cells was dose-dependently increased after levistolide A treatment (Fig. 5c, d). Moreover, the phosphorylation of tau Ser396, Ser416, and Thr181 was significantly decreased in levistolide A–treated N2a/APP695swe cells compared to control cells (Fig. 5e–i). Based on these findings, levistolide A can attenuate the phosphorylation of tau via GSK-3α/β pathways both *in vivo* and *in vitro*.

Levistolide A Regulates the Processing of APP Through Promoting the Activity of PPARγ

To reveal the involvement of PPARγ in APP processing, we first detected the expression of PPARγ in both APP/PS1 Tg

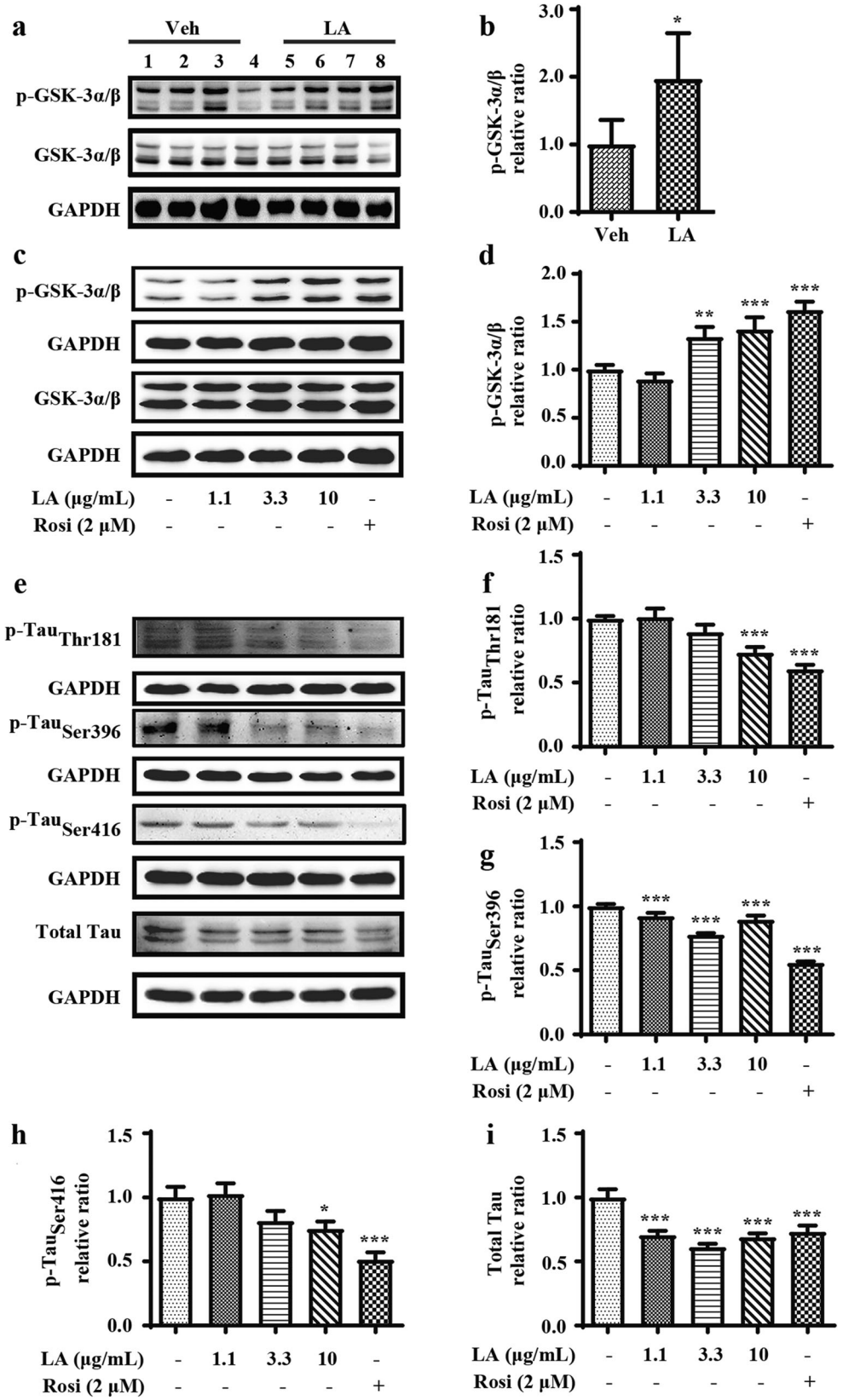

mice and N2a/APP695swe cells. As shown in Fig. 6a and b, the protein level of PPARγ in APP/PS1 Tg mice was elevated by treatment with levistolide A. Similarly, levistolide A also enhanced the protein expression of PPARγ in N2a/

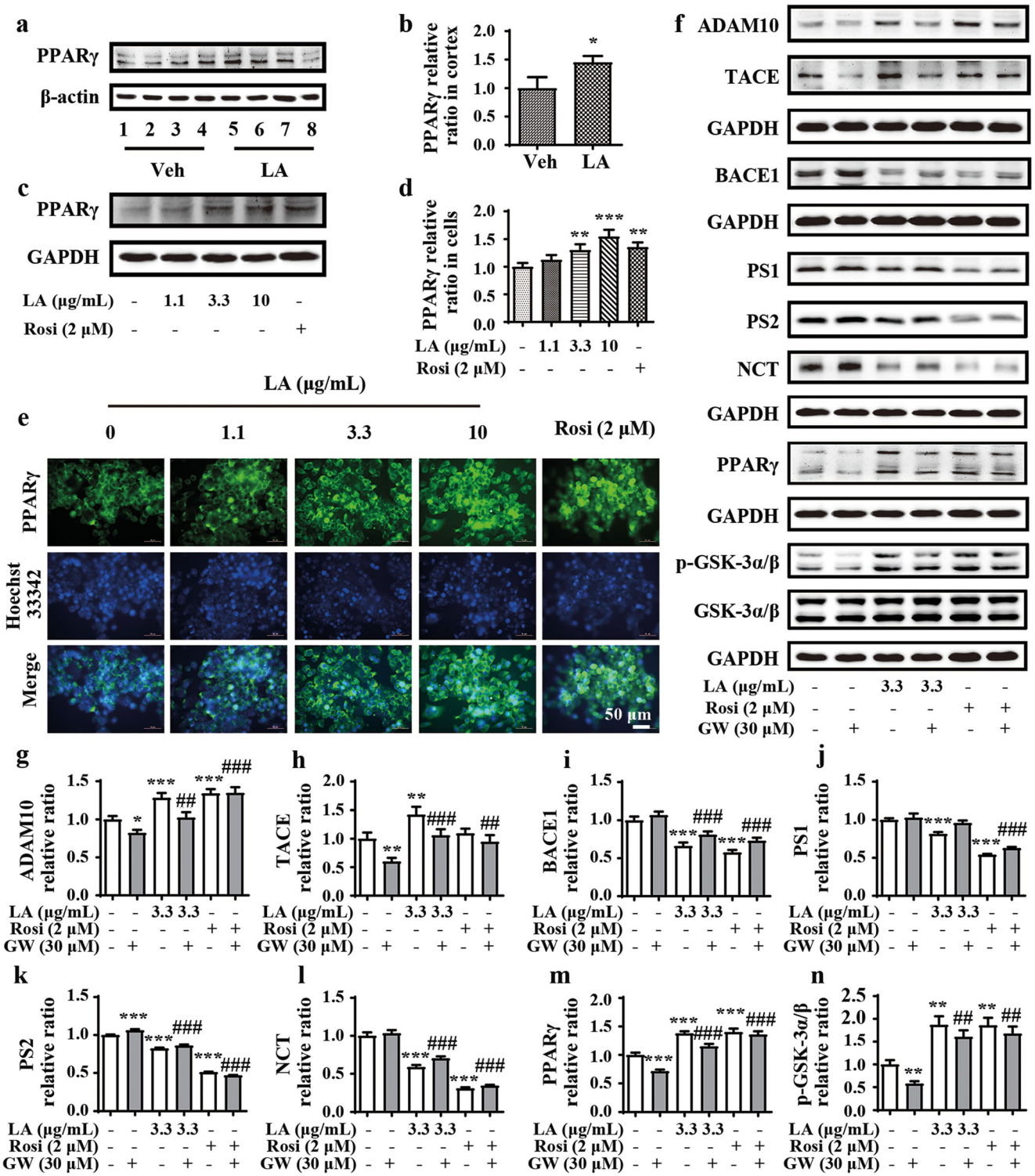

Fig. 6 Levistolide A promoted the activation of PPARγ to regulate APP processing. (a, b) Western blot showing the protein level of PPARγ in the cortex of APP/PS1 Tg mice. β-actin was used as internal control. (c, d) Western blot showing the protein level of PPARγ in the N2a/APP695swe cells. GAPDH was used as internal control. (e) Double-stained immunofluorescence of PPARγ and nuclei in N2a/APP695swe cells, the green fluorescence stands for PPARγ and the blue represents the nuclei. (f) Western blots showing the protein levels including ADAM10, TACE, BACE1, PS1, PS2, NCT, PPARγ, GSK-3α/β, and p-GSK-3α/β. GAPDH was used as internal control. (g–n) Quantitative analysis of the results shown in (f). Data represent the mean ± SD ($n > 3$), *, #$p < 0.05$, **, ##$p < 0.01$, ***, ###$p < 0.001$, compared with the vehicle control

APP695swe cells (Fig. 6c, d). These observations were further confirmed by immunofluorescence staining (Fig. 6e).

To determine whether levistolide A functions in a PPARγ-dependent manner, GW, a selective PPARγ antagonist, was used to treat N2a/APP695swe cells. After 1 h, 30 μM GW treatment partially restored the effects of levistolide A in simultaneously activating α-secretase and suppressing the expression of β- and γ-secretases (Fig. 6f, g–m). In addition, GW reduced the effects of levistolide A on GSK-3α/β phosphorylation, suggesting its role in the phosphorylation of tau.

Overall, we found that levistolide A improved cognitive decline in AD by inhibiting the production and aggregation of Aβ as well as the hyperphosphorylation of tau. Furthermore, PPARγ plays key roles in mediating the effects of levistolide A on the pathogenesis of AD.

Discussion

Neuroprotection is widely accepted as a prospective therapeutic strategy for AD, and increasing evidence has shown that Aβ carries out multiple pathological functions in neurons [12]. As monomeric Aβ can aggregate, the consequent soluble Aβ oligomers showed extreme toxicity to neurons. In fact, a series of studies showed that Aβ oligomer treatment could induce the apoptosis of astrocytes and neurons [37, 38]. Moreover, soluble Aβ plays multiple roles in AD, as for example, it affects oxidative stress, neuroinflammation, and neurotoxicity and inhibits neurogenesis [39, 40]. All of these roles contribute to accelerating the progression of AD. The inhibitory effect of levistolide A on the production of Aβ monomers and oligomers shown based on these clues has revealed its potential therapeutic effect on AD.

Generally, Aβ is produced by the abnormal cleavage of APP by β- and γ-secretases [41]. In contrast, the cleavage of APP by α-secretase is beneficial to for AD [10]. ADAM10 and TACE (or ADAM-17), two α-secretases, cleave APP and play a crucial role in inhibiting Aβ production [42–44]. Increasing evidence has suggested that increased α-secretase contributes to reducing Aβ generation as well as inhibiting tau hyperphosphorylation and synaptic dysfunction [45, 46]. The current investigation expanded upon prior works to reveal the suppressive effect of levistolide A on the formation of APs by increasing the expression of α-secretase. BACE1 and γ-secretases (PS1, PS2, and NCT) play essential roles in producing Aβ via the amyloidogenic metabolism of APP. The downregulation of β- and γ-secretases reduced the production and deposition of Aβ in the brains of AD Tg mice [9, 47, 48]. By these mechanisms, we found that levistolide A decreased the activity of β- and γ-secretases, potentially contributing to the production of Aβ.

Tau functions in stabilizing microtubules, whose hyperphosphorylation is closely related to neuronal loss and cognitive impairment in patients with AD [49–51]. Tau can be phosphorylated at numerous sites, including Ser396, Ser416, and Thr181 [52], resulting in the microtubule disability, leading to the onset of AD [53, 54]. Reciprocally, reducing the phosphorylation of tau may be an effective strategy for AD treatment. The results of our current study demonstrated that the levels of tau phosphorylated at Thr181, Ser396, and Ser416 were decreased in both N2a/APP695swe cells and the cerebral cortices of APP/PS1 Tg mice after exposure to levistolide A. Furthermore, GSK3α/β has been verified to be critical for the phosphorylation of tau [12]. In addition, GSK-3α/β could be activated by sAPPα in an insulin receptor (IR)–activating pathway [55]. The current study demonstrates that levistolide A treatment could increase the production of sAPPα and phosphorylated GSK. Furthermore, levistolide A decreased the hyperphosphorylation of tau, which was possibly related to sAPPα-IR-GSK-3α/β signaling.

Additionally, the deposition of Aβ in APs and phosphorylated tau in NFTs can trigger the inflammatory response during the course of AD development and progression [56]. Furthermore, anti-inflammatory drugs can reduce the pathogenesis of AD [20]. Functional alterations in microglia and astrocytes, the main glial cells in the CNS, contribute to the neuroinflammatory process. On the one hand, microglia, a specific macrophage-like cell type in the CNS, serve as the main immune effector cells in the brain [57, 58]. Under physiological conditions, microglia can eliminate the toxic substances released from damaged cells. However, overactivated microglial cells can induce the neuroinflammatory response by releasing proinflammatory cytokines, which results in cell death, leading to the deposition of Aβ [59, 60]. On the other hand, astrocytes, the most widespread glial cells, exert neuroprotective effects [61, 62]. Overactivated astrocytes can increase the expression of BACE1 and PS1, which generate and deposit Aβ during the course of AD development and progression [63, 64]. In turn, Aβ can activate astrocytes, which produce various cytokines, thus exacerbating neuroinflammatory responses [65]. Therefore, disrupting the crosstalk between Aβ and proinflammatory cytokines might serve as a potential therapeutic strategy to treat AD. Based on this hypothesis, levistolide A treatment effectively inhibited the activation of glial cells and decreased the expression of IL-1β, IL-6, and TNF-α at the protein level in the cerebral cortices of APP/PS1 Tg mice.

PPARγ serves as a transcription factor that regulates the expression of BACE1 [13]. Additionally, PPARγ has been reported to inhibit the accumulation of Aβ by decreasing the release of cytokines by deactivating glial cells [66]. For example, Rosi, a thiazolidinedione (TZD), has neuroprotective effects against Aβ-induced neurodegeneration by inhibiting neuroinflammation [67]. Furthermore, the administration of TZDs can effectively inhibit the deposition of Aβ by downregulating the expression of BACE1 and reducing the

phosphorylation of tau through inhibiting the activity of GSK [68, 69]. In agreement with these results, GW, an antagonist of PPARγ, suppressed the effects of levistolide A in deactivating β- and γ-secretases. To further explore the neuroprotective roles of PPARγ, GW was used to block PPARγ, which clearly decreased the phosphorylation of GSK-3α/β in levistolide A–stimulated N2a/APP695swe cells.

In summary, the present study reveals that treatment with levistolide A can activate PPARγ, which results in the decreased production and aggregation of Aβ by concurrently activating the nonamyloidogenic pathway and deactivating the amyloidogenic pathway as well as reducing the hyperphosphorylation of tau via the GSK3α/β pathway. In addition, neuroinflammation was inhibited by levistolide A. Indeed, AD is a severe neurodegenerative disease caused by multiple etiologies. Many preclinical and experimental studies have demonstrated that the "one-molecule, one-target" (OMOT) strategy has a positive effect in delaying the progression of AD [70, 71]. By targeting multiple AD etiologies, combinatory therapy consisting of more than one drug has shown better therapeutic effects than single drug treatment in clinical practice [72–75]. Considering the multiple targets of levistolide A, it could be a potential and effective drug candidate for rescuing cognitive decline in AD.

Acknowledgments This work was supported by the National Natural Science Foundation of China (Nos. U1608282 and 81771167), the Fundamental Research Funds for the Central Universities, China (No. N172006002), and the Science and Technology Program of Liaoning Province (No. 2019JH2/10300003).

Required Author Forms Disclosure forms provided by the authors are available with the online version of this article.

Author Contributions X. Q. performed the experiments in the study and wrote the manuscript; P. G., L. H., Z. W., and X. H. conceived and designed the research, interpreted the data, and wrote the manuscript.

Compliance with Ethical Standards

Conflict of Interest The authors declare that they have no competing interests.

References

1. Sun JY, Zhang X, Wang C et al. Curcumin decreases hyperphosphorylation of tau by down-regulating Caveolin-1/GSK-3β in N2a/APP695swe cells and APP/PS1 double transgenic Alzheimer's disease mice. Am J Chin Med 2017;45:1667-1682.
2. Xia DY, Huang X, Bi CF et al. PGC-1α or FNDC5 is involved in modulating the effects of $A\beta_{1-42}$ oligomers on suppressing the expression of BDNF, a beneficial factor for inhibiting neuronal apoptosis, Aβ deposition and cognitive decline of APP/PS1 Tg mice. Front Aging Neurosci 2017;9:65.
3. Tian J, Zheng W, Li XL et al. Lower expression of Ndfip1 is associated with Alzheimer disease pathogenesis through decreasing DMT1 degradation and increasing iron influx. Front Aging Neurosci 2018;10:165.
4. Hardy J, Selkoe DJ. The amyloid hypothesis of Alzheimer's disease: progress and problems on the road to therapeutics. Science 2002;297:353-356.
5. Cavallucci V, D'Amelio M, Cecconi F. Aβ toxicity in Alzheimer's disease. Mol Neurobiol 2012;45:366-378.
6. Nunan J, Small DH. Regulation of APP cleavage by α-, β- and γ-secretases. FEBS Lett 2000;483:6-10.
7. Cai W, Yang T, Liu H et al. Peroxisome proliferator-activated receptor γ (PPARγ): A master gatekeeper in CNS injury and repair. Prog Neurobiol 2018;163-164:27-58.
8. Govindarajulu M, Pinky PD, Bloemer J et al. Signaling Mechanisms of Selective PPARγ modulators in Alzheimer's Disease. PPAR Res 2018;2018:1-20.
9. Zhang YW, Thompson R, Zhang H et al. APP processing in Alzheimer's disease. Mol Brain 2011;4:3.
10. Wang Z, Huang XS, Zhao P et al. Catalpol inhibits amyloid-β generation through promoting α-cleavage of APP in swedish mutant APP overexpressed N2a cells. Front Aging Neurosci 2018;10:66.
11. Ohno M, Cole SL, Yasvoina M et al. BACE1 gene deletion prevents neuron loss and memory deficits in 5XFAD APP/PS1 transgenic mice. Neurobiol Dis 2007;26:134-145.
12. Yankner BA. Mechanisms of neuronal degeneration in Alzheimer's disease. Neuron 1996;16:921-932.
13. Lin N, Chen LM, Pan XD et al. Tripchlorolide attenuates β-amyloid generation via suppressing PPARγ-regulated BACE1 activity in N2a/APP695 cells. Mol Neurobiol 2016;53:6397-6406.
14. Luo DZ, Hou XY, Hou L et al. Effect of pioglitazone on altered expression of Aβ metabolism-associated molecules in the brain of fructose-drinking rats, a rodent model of insulin resistance. Eur J Pharmacol 2011;664:14-19.
15. Mietelska-Porowska A, Wasik U, Goras M et al. Tau protein modifications and interactions: their role in function and dysfunction. Int J Mol Sci 2014;15:4671-4713.
16. Liu F, Liang ZH, Shi JH et al. PKA modulates GSK-3β- and cdk5-catalyzed phosphorylation of tau in site- and kinase-specific manners. FEBS Lett 2006;580:6269-6274.
17. Inestrosa NC, Godoy JA, Quintanilla RA et al. Peroxisome proliferator-activated receptor γ is expressed in hippocampal neurons and its activation prevents β-amyloid neurodegeneration: role of Wnt signaling. Exp Cell Res 2005;304:91-104.
18. Tang XL, Wang CN, Zhu XY et al. Rosiglitazone inhibition of calvaria-derived osteoblast differentiation is through both of PPARγ and GPR40 and GSK3β-dependent pathway. Mol Cell Endocrinol 2015;413:78-89.
19. Liu JJ, Dai XJ, Xu Y et al. Inhibition of lymphoma cell proliferation by peroxisomal proliferator-activated receptor-γ ligands via Wnt signaling pathway. Cell Biochem Biophys 2012;62:19-27.
20. Bagyinszky E, Giau VV, Shim K et al. Role of inflammatory molecules in the Alzheimer's disease progression and diagnosis. J Neurol Sci 2017;376:242-254.
21. McNaull BB, Todd S, McGuinness B et al. Inflammation and anti-inflammatory strategies for Alzheimer's disease. Gerontology 2010;56:3-14.
22. Kapadia R, Yi JH, Vemuganti R. Mechanisms of anti-inflammatory and neuroprotective actions of PPAR-γ agonists. Front Biosci 2008;13:1813-1826.
23. Lenglet S, Montecucco F, Mach F. Role of matrix metalloproteinases in animal models of ischemic stroke. Curr Vasc Pharmacol 2015;13:161-166.
24. Heneka MT, Klockgether T, Feinstein DL. Peroxisome proliferator-activated receptor-γ ligands reduce neuronal inducible nitric oxide synthase expression and cell death *in vivo*. J Neurosci 2000;20:6862-6867.

25. Calhoun ME, Burgermeister P, Phinney AL et al. Neuronal overexpression of mutant amyloid precursor protein results in prominent deposition of cerebrovascular amyloid. Proc Natl Acad Sci U S A 1999;96:14088-14093.
26. Kuang X, Du JR, Liu YX et al. Postischemic administration of Z-Ligustilide ameliorates cognitive dysfunction and brain damage induced by permanent forebrain ischemia in rats. Pharmacol Biochem Behav 2008;88:213-221.
27. Peng HY, Du JR, Zhang GY et al. Neuroprotective effect of Z-ligustilide against permanent focal ischemic damage in rats. Biol Pharm Bull 2007;30:309-312.
28. Noda T, Shiga H, Yamada K et al. Effects of tokishakuyakusan on regeneration of murine olfactory neurons *in vivo* and *in vitro*. Chem Senses 2019;44:327-338.
29. Zhang T, Ding Y, An H et al. Screening anti-tumor compounds from Ligusticum wallichii using cell membrane chromatography combined with high-performance liquid chromatography and mass spectrometry. J Sep Sci 2015;38:3247-3253.
30. Choi HG, Je IG, Kim GJ et al. Chemical constituents of the root of *Angelica* tenuissima and their anti-allergic inflammatory activity. Nat Prod Commun 2017;12:779-780.
31. Velazquez-Moyado JA, Martinez-Gonzalez A, Linares E et al. Gastroprotective effect of diligustilide isolated from roots of Ligusticum porteri coulter & rose (Apiaceae) on ethanol-induced lesions in rats. J Ethnopharmacol 2015;174:403-409.
32. Guo C, Wang T, Zheng W et al. Intranasal deferoxamine reverses iron-induced memory deficits and inhibits amyloidogenic APP processing in a transgenic mouse model of Alzheimer's disease. Neurobiol Aging 2013;34:562-575.
33. Zhang FJ, Jiang LL. Neuroinflammation in Alzheimer's disease. Neuropsychiatr Dis Treat 2015;11:243-256.
34. Wang Y, Xia J, Shen MJ et al. Effects of bis-mep on reversing amyloid plaque deposition and spatial learning and memory impairments in a mouse model of β-amyloid peptide- and ibotenic acid-induced Alzheimer's disease. Front Aging Neurosci 2019;11:3.
35. Paudel P, Seong SH, Zhou YJ et al. Rosmarinic acid derivatives' inhibition of glycogen synthase kinase-3β is the pharmacological basis of kangen-karyu in Alzheimer's disease. Molecules 2018;23:2919.
36. Hooshmandi E, Ghasemi R, Iloun P et al. The neuroprotective effect of agmatine against amyloid β-induced apoptosis in primary cultured hippocampal cells involving ERK, Akt/GSK-3β, and TNF-α. Mol Biol Rep 2019;46:489-496.
37. Balducci C, Forloni G. Doxycycline for Alzheimer's Disease: Fighting β-amyloid oligomers and neuroinflammation. Front Pharmacol 2019; 10:738.
38. Wilkaniec A, Gassowska-Dobrowolska M, Strawski M et al. Inhibition of cyclin-dependent kinase 5 affects early neuroinflammatory signalling in murine model of amyloid beta toxicity. J Neuroinflammation 2018; 15:1.
39. Forloni G, Balducci C. Alzheimer's Disease, Oligomers, and Inflammation. J Alzheimers Dis 2018; 62:1261-1276.
40. Jeong S. Molecular and cellular basis of neurodegeneration in Alzheimer's Disease. Mol Cell 2017; 40:613-620.
41. Crump CJ, Johnson DS, Li YM. Development and mechanism of γ-secretase modulators for Alzheimer's disease. Biochemistry 2013;52:3197-3216.
42. Kuhn PH, Wang HH, Dislich B et al. ADAM10 is the physiologically relevant, constitutive α-secretase of the amyloid precursor protein in primary neurons. EMBO J 2010;29:3020-3032.
43. Scheller J, Chalaris A, Garbers C et al. ADAM17: a molecular switch to control inflammation and tissue regeneration. Trends Immunol 2011;32:380-387.
44. Saftig P, Reiss K. The "a disintegrin and metalloproteases" ADAM10 and ADAM17: novel drug targets with therapeutic potential? Eur J Cell Biol 2011;90:527-535.
45. Sun M, Zhou T, Zhou L et al. Formononetin protects neurons against hypoxia-induced cytotoxicity through upregulation of ADAM10 and sAβPPα. J Alzheimers Dis 2012;28:795-808.
46. Pruessmeyer J, Ludwig A. The good, the bad and the ugly substrates for ADAM10 and ADAM17 in brain pathology, inflammation and cancer. Semin Cell Dev Biol 2009;20:164-174.
47. Ahn K, Shelton CC, Tian Y et al. Activation and intrinsic γ-secretase activity of presenilin 1. Proc Natl Acad Sci U S A 2010;107:21435-21440.
48. Baulac S, LaVoie MJ, Kimberly WT et al. Functional γ-secretase complex assembly in Golgi/*trans*-Golgi network: interactions among presenilin, nicastrin, Aph1, Pen-2, and γ-secretase substrates. Neurobiol Dis 2003;14:194-204.
49. Zhang ZX, Zhao RP, Qi JP et al. Inhibition of glycogen synthase kinase-3β by *Angelica sinensis* extract decreases β-amyloid-induced neurotoxicity and tau phosphorylation in cultured cortical neurons. J Neurosci Res 2011;89:437-447.
50. Khan SS, Bloom GS. Tau: the center of a signaling nexus in Alzheimer's disease. Front Neurosci 2016;10:31.
51. Gao Y, Tan L, Yu JT et al. Tau in Alzheimer's disease: mechanisms and therapeutic strategies. Curr Alzheimer Res 2018;15:283-300.
52. Fontaine SN, Sabbagh JJ, Baker J et al. Cellular factors modulating the mechanism of tau protein aggregation. Cell Mol Life Sci 2015;72:1863-1879.
53. Li T, Paudel HK. Glycogen synthase kinase 3β phosphorylates Alzheimer's disease-specific Ser^{396} of microtubule-associated protein tau by a sequential mechanism. Biochemistry 2006;45:3125-3133.
54. Milenkovic I, Jarc J, Dassler E et al. The physiological phosphorylation of tau is critically changed in fetal brains of individuals with Down syndrome. Neuropathol Appl Neurobiol 2018;44:314-327.
55. Jimenez S, Torres M, Vizuete M et al. Age-dependent accumulation of soluble amyloid β (Aβ) oligomers reverses the neuroprotective effect of soluble amyloid precursor protein-α (sAPPα) by modulating phosphatidylinositol 3-kinase (PI3K)/Akt-GSK-3β pathway in Alzheimer mouse model. J Biol Chem 2011; 286:18414-18425.
56. Hoesel B, Schmid JA. The complexity of NF-κB signaling in inflammation and cancer. Mol Cancer 2013;12:86.
57. Perry VH, Teeling J. Microglia and macrophages of the central nervous system: the contribution of microglia priming and systemic inflammation to chronic neurodegeneration. Semin Immunopathol 2013;35:601-612.
58. Cai ZY, Hussain MD, Yan LJ. Microglia, neuroinflammation, and β-amyloid protein in Alzheimer's disease. Int J Neurosci 2014;124:307-321.
59. Hickman SE, Allison EK, El Khoury J. Microglial dysfunction and defective β-amyloid clearance pathways in aging Alzheimer's disease mice. J Neurosci 2008;28:8354-8360.
60. Chen W, Liang TT, Zuo WW et al. Neuroprotective effect of 1-Deoxynojirimycin on cognitive impairment, β-amyloid deposition, and neuroinflammation in the SAMP8 mice. Biomed Pharmacother 2018;106:92-97.
61. Burda JE, Bernstein AM, Sofroniew MV. Astrocyte roles in traumatic brain injury. Exp Neurol 2016;275:305-315.
62. Sofroniew MV, Vinters HV. Astrocytes: biology and pathology. Acta Neuropathol 2010;119:7-35.
63. Zhao J, O'Connor T, Vassar R. The contribution of activated astrocytes to Aβ production: implications for Alzheimer's disease pathogenesis. J Neuroinflammation 2011;8:150.
64. Patil S, Sheng LF, Masserang A et al. Palmitic acid-treated astrocytes induce BACE1 upregulation and accumulation of C-terminal fragment of APP in primary cortical neurons. Neurosci Lett 2006;406:55-59.
65. Burkert K, Moodley K, Angel CE et al. Detailed analysis of inflammatory and neuromodulatory cytokine secretion from human NT2

astrocytes using multiplex bead array. Neurochem Int 2012;60:573-580.
66. Yamanaka M, Ishikawa T, Griep A et al. PPARγ/RXRα-induced and CD36-mediated microglial amyloid-β phagocytosis results in cognitive improvement in amyloid precursor protein/presenilin 1 mice. J Neurosci 2012;32:17321-17331.
67. De Felice FG, Vieira MN, Bomfim TR et al. Protection of synapses against Alzheimer's-linked toxins: insulin signaling prevents the pathogenic binding of Aβ oligomers. Proc Natl Acad Sci U S A 2009;106:1971-1976.
68. Yoon SY, Park JS, Choi JE et al. Rosiglitazone reduces tau phosphorylation via JNK inhibition in the hippocampus of rats with type 2 diabetes and tau transfected SH-SY5Y cells. Neurobiol Dis 2010;40:449-455.
69. Escribano L, Simon AM, Gimeno E et al. Rosiglitazone rescues memory impairment in Alzheimer's transgenic mice: mechanisms involving a reduced amyloid and tau pathology. Neuropsychopharmacology 2010;35:1593-1604.
70. combination therapy as multi-targets strategy to combat Alzheimer's disease. J Ethnopharmacol 2018; 215:42-73.
71. Mangialasche F, Solomon A, Winblad B, Mecocci P, Kivipelto M. Alzheimer's disease: clinical trials and drug development. Lancet Neurol 2010; 9:702-716.
72. Fessel J. Prevention of Alzheimer's disease by treating mild cognitive impairment with combinations chosen from eight available drugs. Alzheimers Dement (N Y) 2019; 5:780-788.
73. Gauthier S, Molinuevo JL. Benefits of combined cholinesterase inhibitor and memantine treatment in moderate-severe Alzheimer's disease. Alzheimers Dement 2013; 9:326-331.
74. Joe E, Ringman JM. Cognitive symptoms of Alzheimer's disease: clinical management and prevention. BMJ 2019; 367:l6217.
75. Patel L, Grossberg GT. Combination therapy for Alzheimer's disease. Drugs Aging 2011; 28:539-546.